Biophysical Journal Volume 104 May 2013 2193–2201

Interfacial Properties of High-Density Lipoprotein-like Lipid Droplets with Different Lipid and Apolipoprotein A-I Compositions

Artturi Koivuniemi,[†*] Marko Sysi-Aho,[†] Matej Orešič,[†] and Samuli Ollila[‡]
[†]VTT Bio- and Chemical Processes, Espoo, Finland; and [‡]Physical Chemistry, Lund University, Lund, Sweden

ABSTRACT The surface properties of high-density lipoproteins (HDLs) are important because different enzymes bind and carry out their functions at the surface of HDL particles during metabolic processes. However, the surface properties of HDL and other lipoproteins are poorly known because they cannot be directly measured for nanoscale particles with contemporary experimental methods. In this work, we carried out coarse-grained molecular dynamics simulations to study the concentration of core lipids in the surface monolayer and the interfacial tension of droplets resembling HDL particles. We simulated lipid droplets composed of different amounts of phospholipids, cholesterol esters (CEs), triglycerides (TGs), and apolipoprotein A-Is. Our results reveal that the amount of TGs in the vicinity of water molecules in the phospholipid monolayer is 25–50% higher compared to the amount of CEs in a lipid droplet with a mixed core of an equal amount of TG and CE. In addition, the correlation time for the exchange of molecules between the core and the monolayer is significantly longer for TGs compared to CEs. This suggests that the chemical potential of TG is lower in the vicinity of aqueous phase but the free-energy barrier for the translocation between the monolayer and the core is higher compared to CEs. From the point of view of enzymatic modification, this indicates that TG molecules are more accessible from the aqueous phase. Further, our results point out that CE molecules decrease the interfacial tension of HDL-like lipid droplets whereas TG keeps it constant while the amount of phospholipids varies.

INTRODUCTION

High-density lipoprotein (HDL) particles play an important role in the reverse cholesterol transport (RCT) (1). In this process, cholesterol and other lipid molecules are transported from extrahepatic tissues to the liver. The efficiency of RCT, especially the HDL-mediated cholesterol efflux from arterial wall lipid-laden macrophages, is thought to be important in the prevention of coronary heart disease (2). Because the effectiveness of RCT is tightly linked to the rate of different enzymatic processes, it is important to understand the key regulatory mechanisms behind these processes. Because many enzymes and proteins involved in the lipoprotein metabolism carry out their function at the lipoprotein droplet surfaces (3), it is likely that the surface properties of HDL particles play an important role in these processes.

Spherical HDL particles are composed of a hydrophobic core (containing cholesterol esters (CEs), triglycerides (TGs), and a small amount of unesterified cholesterol), which is covered by an amphiphilic monolayer comprised of phospholipids, cholesterol, and different apolipoproteins, with the main protein component being apolipoprotein A-I (apoA-I). The diameter of spherical HDL particles is ranging from 7 to 12 nm (1).

In this work, we focus on two important surface properties of HDL-like lipid droplets: the concentration of core lipids in the surface monolayer and the interfacial tension. The amount of core lipids in the interfacial monolayer is an important regulatory factor regarding enzymes that transfer or modify core lipids, like cholesteryl ester transfer protein (CETP) and different lipases. On the other hand, the adsorption of proteins at the interface (4,5) and the amount of core lipids (6–8) can be regulated by changing the surface pressure (interfacial tension). Interfacial tension is also related to the shape and stability of lipid droplets as recently discussed in Ollila et al. (9). Consequently, it is obvious that these properties are very interesting in regard to understanding the functionality of HDL in the RCT. In addition to lipoproteins, the surface properties of cytosolic lipid droplets play an important role, e.g., in cholesteryl ester lipolysis, which has been recognized as a rate-limiting step in the cholesterol efflux from macrophages (10).

These properties are very difficult to study experimentally in nanometer-sized lipid droplets, but similar macroscopical interfaces can be studied, for example, with droplet tensiometer and Langmuir troughs (4,6,11). Also, measurements for vesicles and emulsion particles can be exploited to understand the features of nanoscale lipid droplets (12,13). However, it is not known how well the experimental conditions in the above-mentioned systems reflect the behavior of lipids in highly curved nanoscale lipoprotein particles with molecular composition regulated by physiological processes. For example, the binding of human apolipoproteins E3 and E4 to an emulsion droplet surface has been shown to be dependent on the particle size (14). These issues are discussed in a recent molecular dynamics simulation study concerning interfacial tension (9).

In this work, we use coarse-grained molecular dynamics simulations to study the influence of core composition and presence of apoA-Is on the interfacial tension, and the core lipid concentration in the monolayer. Thanks to the

Submitted July 16, 2012, and accepted for publication February 14, 2013.
*Correspondence: artturi.koivuniemi@vtt.fi
Editor: Reinhard Lipowsky.

0006-3495/13/05/2193/9 $2.00
http://dx.doi.org/10.1016/j.bpj.2013.02.058

recent development in molecular dynamics simulation methodologies, it is computationally efficient to run coarse-grained simulations of HDL-like lipid droplets (15–17). Furthermore, we can now computationally calculate the interfacial tensions for spherical droplets (9,18).

We simulated HDL-like lipid droplets composed of 1-palmitoyl-2-oleoyl-*sn*-glycero-3-phosphocholine (POPC), TG (18:1,18:1,18:1), and CE (18:2) molecules. We systematically increased the number of surfactant lipids with different CE/TG ratio in the core and analyzed the interfacial concentrations of core lipids and interfacial tensions. In addition, we analyzed the effect of embedding two and four apoA-Is at the interface. According to our results, the solubility of TG to the interface is higher compared to CE, which makes TGs more accessible for enzymatic modifications. Furthermore, we found that interfacial tension is less dependent on POPC amount when TG is present in the core. For this reason, the interfacial tension increases when CE:TG ratio in the core decreases. We also found that the addition of the first two apoA-Is to the CE-POPC particle lowers the interfacial tension only slightly, but the addition of the third and the fourth apoA-Is has a more drastic effect.

MATERIALS AND METHODS

Simulation details

To begin, we constructed initial configurations for lipid droplets without apoA-Is by adding or removing lipids from the previously simulated HDL particle models (19). Then the lipids were solvated with 10,000 water beads, which was followed by 500-step energy minimizations. With this procedure, systems with CE/TG ratios of 1:0, 1:1, and 0:1 in the core were constructed. These cores were surrounded by 0, 60, 100, or 140 POPC molecules. Subsequently, all systems were simulated up to 5 μs (effective MARTINI time, i.e., the real simulation time is multiplied by 4 (15), the total number of simulation steps was 62,500,000, and the timestep was set to 0.02 ps). The systems were labeled as S0–S9 and the number of molecules in each simulation are displayed in Table 1. As an example, the end configuration snapshots from simulations S5 and S7 are shown in Fig. 1.

TABLE 1 System composition, radii of gyration (R_g (nm)), Laplace radii (R_s (nm)), interfacial tensions (γ_s (mN/m)), and water-accessible hydrophobic surface for the simulations (SAHA (nm^2))

System	CE	TG	POPC	apoA-I	R_g	R_L	γ	SAHA
S0	80	0	0	0	2.1	2.7	36	122
S1	80	0	60	0	2.7	3.7	31	70
S2	80	0	100	0	3.0	4.0	30	51
S3	80	0	140	0	3.2	4.6	23	38
S4	40	40	0	0	2.3	2.9	36	121
S5	40	40	60	0	2.8	3.7	33	73
S6	40	40	100	0	3.1	4.0	31	56
S7	40	40	140	0	3.3	4.3	28	43
S8	0	80	0	0	2.5	3.0	31	124
S9	0	80	140	0	3.4	4.4	32	41
SP2	80	0	100	2	3	3.8	25	29
SP4	80	0	100	4	3	4.0	15	28

In addition, we carried out simulations containing two or four apoA-Is embedded in the lipid droplet with 100 POPC molecules and CE/TG ratio of 1:0 in the core. The apoA-I model (amino acids 40–243 of apoA-I) is based on the recently published structure of the trefoil model around spherical HDL particles (20). The structure for the trefoil model of apoA-I is available in the Protein Model Database (http://mi.caspur.it/PMDB/) with accession No. PM0075240. One apoA-I was added to the trefoil model in 5:5 registry fashion (see the Supporting Material) to produce a tetrafoil model of apoA-Is. The reason for the incorporation of an additional apoA-I was that, on average, spherical HDL particles consist of four apoA-Is (20). The atomistic tetrafoil model of the apoA-Is was then coarse-grained. The secondary structure of apoA-I was mostly α-helical, but proline residues and amino acids next to prolines were modeled as random coil structures. The coarse-grained tetrafoil model of apoA-Is was placed around the lipid droplet with 100 POPCs and 80 CLs (system S2). Next, 500-step energy minimization and short vacuum simulation were carried out to get the apoA-Is attached to the lipid droplet surface. A quantity of 20,000 water beads was added to the system after which the system was simulated up to 5 μs. We refer to the apoA-I system as SP4. At the end of SP4 simulation, two apoA-Is were removed from the system and the system with two apoA-Is (SP2) was simulated for 5 μs.

We used VMD (21) in the construction of the simulation systems, GROMACS 4 (22) and the MARTINI force field (15,16), in all the simulations. The model for POPC is part of the standard MARTINI force field (15). Models for CE and TG were constructed from MARTINI building blocks, as described in Vuorela et al. (17). The extension of MARTINI for proteins (16) was used to model apoA-Is.

All systems were considered equilibrated after 2 μs when no drifting in molecular contacts occurred. The Berendsen coupling scheme with coupling constant of 1.0 ps^{-1} was used to set the temperature to 320 K and couple pressure isotropically to 1.0 bar (23). The core of the native HDL particles is assumed to be in a liquid state. To ensure that this is the case also in our simulations with pure CE cores, we have chosen the simulation temperature of 320 K, which is above the melting temperature of CE (18:2) (24). Cutoffs for Lennard-Jones and electrostatic interactions were set to 1.2 nm. In Lennard-Jones interactions, shift function was introduced at 0.9 nm. These are standard parameters of the MARTINI force field (15,16).

Analysis methods

The three-dimensional radial number density of lipid molecules was determined by the g_rdf program included in the GROMACS package (22). To calculate the amount of CEs and TGs solubilized to phospholipids, we calculated the number of contacts between the polar beads of CEs (the ES bead) or TGs (the GLY bead) and water beads. The number of polar groups of core lipids located closer than 0.75 nm from the nearest water bead was calculated by using the g_mindist program available in the GROMACS simulation package. The cutoff 0.75 nm was chosen because the distance distribution between water and ES or GLY beads had two distinct peaks corresponding to the interfacial and the core region. The minimum between these two peaks is located at the 0.75 nm that was chosen to separate the interfacial and the core regions. The radius of gyrations R_g were calculated using the g_gyrate program included in the GROMACS package and all lipids were included in the calculations. Order parameters for POPC acyl chain beads were defined as

$$S_n = \frac{3}{2}\langle \cos^2\theta_n \rangle - \frac{1}{2}, \quad (1)$$

where θ_n is the angle between the vector from bead n−1 to n+1 and the normal of the droplet. This was done with the g_order program included in the GROMACS package.

The Laplace radii and interfacial tensions were calculated by using its connection to local pressure as described in Ollila et al. (9). Briefly, we

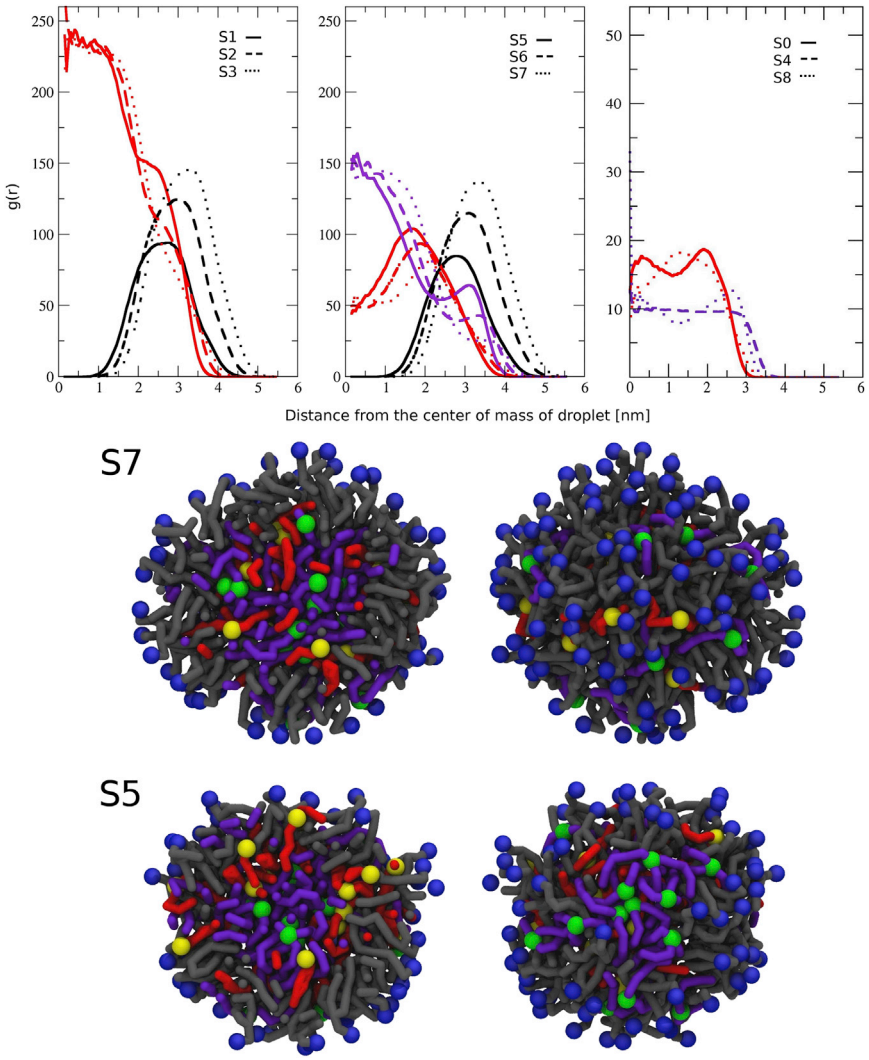

FIGURE 1 Radial density profiles showing the distribution of core and surface lipids in lipid droplet simulations S0-S8 (*above*). (*Black* refers to POPC, *red* to CE, and *purple* to TG.) Snapshots from the end of simulations of S5 and S7 to visualize the distribution of core lipids in lipid droplets when surface pressure is increased (*bottom*). (*Left simulation snapshots*) Slice from the center of particles. (*Right snapshots*) Surface of droplets. (*Gray sticks*) POPC molecules. (*Blue spheres*) NC3 beads. (*Red*) Cholesterol esters. (*Indigo*) Triglycerides. (*Green spheres*) GLY (TG) beads. (*Yellow spheres*) ES (CE) beads. For clarity, the water beads were removed from the snapshots.

divided the system into a grid (with a spacing of 0.2 nm), calculated the local pressure tensor in each cube in the grid, transformed the tensor in every cube to spherical coordinates, and then averaged over angular coordinates to find transverse $p_T(r)$ and normal $p_{rr}(r)$ components of pressure tensor as a function of radial distance from the center of mass (18). Then equations

$$\gamma_s = -\int_0^\infty \left(\frac{r}{R_s}\right)^2 [p_T(r) - p_{rr}(r)]\mathrm{d}r \tag{2}$$

and

$$R_s^3 = \frac{\int_0^\infty r^2[p_T(r) - p_{rr}(r)]\mathrm{d}r}{\int_0^\infty r^{-1}[p_T(r) - p_{rr}(r)]\mathrm{d}r} \tag{3}$$

were used to calculate Laplace radius and the interfacial tension. The core was assumed to be bulk when $r < 1.0$ nm for all the systems expected for the system S0 when $r < 0.5$ nm. In bulk $p_T(r) = p_{rr}(r)$, the integrand in Eqs. 2 and 3 is zero. The error bars, calculated by varying this location by 1 nm, were ± 3 for SO and ± 1 for the rest of the systems. For more details and discussion, see Ollila et al. (9).

The surface pressure $\Pi(A)$ is defined to be the reduction of interfacial tension due to the presence of interfacial monolayer

$$\Pi(A) = \gamma_0 - \gamma(A), \tag{4}$$

where γ_0 is the interfacial tension without surfactants. Note that in this description the interfacial tension with surfactant (and surface pressure) depends on the area per surfactant A. This corresponds to a situation where the number of surfactant molecules at the interface is constant when the area is changing. This assumption is reasonable if the exchange rate of molecules between interface and bulk is slower than the timescale of the studied phenomena. This is a plausible situation in physiological lipid droplets because the exchange rate for phospholipids with long tail (>12 carbons) is very slow (several hours) (25), which is much slower compared to the modification rates of enzymes. In this work, the interfacial tension always refers to the Laplace interfacial tension, which satisfies the Laplace equation with the Laplace radius.

To estimate the exchange rates for lipid molecules between interfacial region and core region, we defined a normalized correlation function

$$C_i(\tau) = \frac{\langle H_i(t)H_i(t+\tau)\rangle_t}{\langle H_i(t)^2\rangle_t}, \quad (5)$$

where $H_i(t)$ is a binary function having the value of 1, when the distance between water and polar bead of a lipid (GLY for TG,ES for CE) is $\leq$0.75 nm, and the value of 0 otherwise. This correlation time will decay to zero after the time τ when all the polar beads, which were in the interface at the time t, are transported to the core. Then the correlation time τ_c for the transport was calculated by integrating $C_i(\tau)$,

$$\tau_c = \int_0^\infty C_i(\tau)\mathrm{d}\tau. \quad (6)$$

The solvent-accessible hydrophobic surface area (SAHA) was calculated by using the g_sas program included in the GROMACS package (22). All acyl-chain and sterol carbon superatoms (beads) were considered as hydrophobic beads. Headgroups and ester-bond regions of lipids were classified as hydrophilic. The radius of the solvent probe was set to 0.43 nm.

RESULTS AND DISCUSSION

Distribution of core lipids

Radial density profiles with respect to the center of mass of lipid droplets are shown in Fig. 1. The radial density profiles show significantly different behavior for CE and TG in the core and interfacial regions.

In the mixed core lipid systems, CE concentrates next to the phospholipid region in the core, wheras TG molecules fills the innermost part. This result can be interpreted as an indication of microphase separation of the core into TG inner core and CE outer core layers, as suggested previously by Pregetter et al. (26) in the case of LDL particles. On the other hand, the amount of TGs at the water-phospholipid interface is higher when compared to CEs as seen from the other density maximum in the monolayer region. These features are also present but less pronounced in previous simulations studies due to the lower relative amount of TG (17,19,27).

The accessibility of core lipids from the aqueous phase is important, e.g.. for the activity of CETP, and different lipases' hydrolyzing core lipids. To estimate the accessibility, we calculated the number of polar groups for each core lipid located closer than 0.75 nm from the nearest water molecule. The results are shown in Fig. 2. The number of polar beads in the vicinity of water molecules is ~25–50% higher for TG compared to CEs in the system with the mixed core. This is in accordance with the density profiles in Fig. 1 and emulsion particle experiments where the amount of TGs at the surface was reported to be twice the amount of CEs (12). The number of polar groups in the vicinity of water always decreases for core molecules when POPC is added. Interestingly, the decrease is more pronounced for TG than CE in the system with the mixed core. This is in accordance

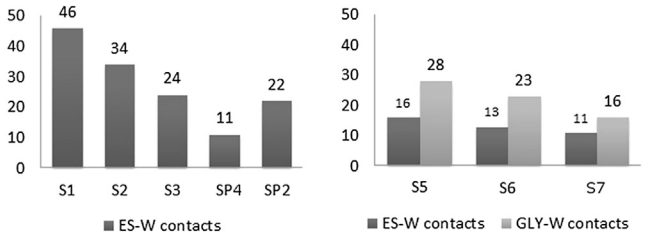

FIGURE 2 Number of contacts between core lipid ES (CE) or GLY (TG) beads and water beads. The standard deviations for the number of contacts are two.

with the changes in the density profile where the second maximum of TG density is decreasing in the monolayer region when the amount of POPC is increasing. In the pure TG core system S9, the number of surface-located TGs was 33 (data not shown), indicating that CEs can replace ~30% of TGs at the surface when the amount and type of the surface-located core lipids are considered in systems S9 and S7. It should be noted that the presence of free cholesterol might influence these results because the addition of cholesterol to a lipid bilayer decreases the solubility of TGs, whereas in the case of CEs the effect of cholesterol is smaller (28,29).

Density distributions are similar also in the mixed droplet without surfactant in a sense that TG has a local density maximum close to the water-lipid interface and CE concentrates in the layer just below interfacial TG. The preference of TG molecules to locate at the interface could be explained by a higher polarity or a lower structural energy of a molecule at the interface. The minor differences in the SAHAs between TG and CE systems, shown in Table 1, do not support the first option. The higher interfacial energy for CE could arise, for example, from energetically unfavored horseshoe-like conformation at the interface (7,30). Because our main focus is in HDL-like droplets containing phospholipid monolayer, we do not analyze this further.

The different behavior between TG and CE in the presence of phospholipids is probably related to the interactions with TG/CE and phospholipids. To analyze the effect of core lipids on POPC monolayer, we calculated the order parameters of acyl-chain beads. The results for S1–S6, SP, and SP2 systems are shown in Fig. 3. The order parameters are clearly increasing with increased amount of POPC at the interface when only CE is present in the core. With the mixed TG/CE core, the order parameters are essentially unchanged with increasing amount of POPC. Generally, order parameters are higher or equal in the system with mixed core compared to the pure CE core. These results suggest that the TG has a stronger ordering effect on POPC monolayer especially with lower POPC concentrations. Our results can be interpreted such that intrinsically TG prefers to be at the interface, but in the presence of POPC it is pushed away due to decreased entropy the of POPC monolayer.

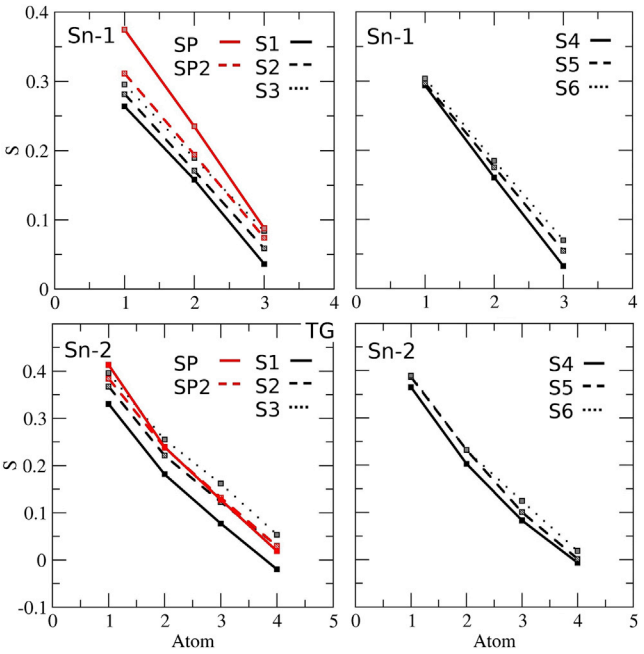

FIGURE 3 Order parameters for POPC acyl chains in simulations S1–S6, SP2, and SP4. (*Black lines*) Pure lipid droplet simulations. (*Red lines*) Simulations in which apo A-Is are also present.

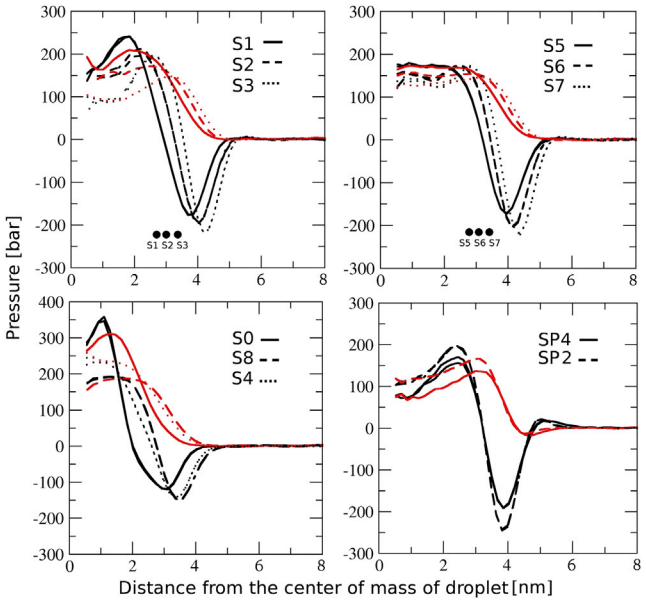

FIGURE 4 Pressure profiles for lipid droplets in simulations: S1–S3, S5–S7, S0, S4, S8, SP2, and SP4. (*Black lines*) Transverse $p_T(r)$. (*Red lines*) Normal $p_{rr}(r)$ components of the pressure. (*Black points*) POPC density maxima, which are taken from the data in Fig. 1.

Effect of lipid composition on interfacial tension

Interfacial tensions for simulated droplets were calculated by using pressure profiles as described in Materials and Methods and in Ollila et al. (9). Calculated pressure profiles and interfacial tensions for droplets with different core compositions are shown in Fig. 4 and Table 1, respectively. The calculated TG-water interfacial tension 31 ± 1 mN/m (system S8) is in good agreement with the experimental value 32 mN/m (31), as already shown in Ollila et al. (9). The calculated interfacial tension for both the pure CE droplet (system S0) and the mixed CE/TG droplet (system S4) was 36 mN/m, which is somewhat larger compared to the pure TG droplet. Seemingly similar values for the pure CE system and the mixed one might be due to a nontrivial surface behavior of molecules or a relatively large error bar (±3 mN/m) for the pure CE system. In the only experimental measurement for interfacial tension of the CE-containing systems, the interfacial tension was essentially unchanged when small amounts (<4 wt %) of CE were added into triolein (32).

From Table 1 we see that the interfacial tension decrease due to the addition of surfactant phospholipids (POPC) depends on the core lipid composition. The higher the relative concentration of CE, the stronger was the observed decrease. For example, the interfacial tension decrease due to the addition of 140 POPC molecules was 13 mN/m and 8 mN/m with the CE and the mixed TG/CE cores, respectively, whereas with pure TG core there was essentially no decrease. On the other hand, by comparing systems S3, S7, and S9, we observed a clear increase in interfacial tension when CEs were replaced by TGs in the core whereas the amount of POPCs was unchanged. In all, our results indicate that CEs lower the interfacial tension, whereas TGs reduce the changes due to monolayer composition changes. This would also indicate that CEs render droplets more stable with all surface compositions whereas TG buffers the interfacial property changes caused by the modifications in monolayer composition.

The buffering effect of TG is already suggested in recent experimental work, in which interfacial tension change due to area per PC change was found to be very small in the area per molecule region where TG is escaping from the monolayer (6). Our simulations are in agreement with this picture because the second maximum of TG density profile in the monolayer region decreases when POPC amount is increased, whereas much lower variations are found in the CE density profile. In conclusion, we suggest that TG molecules leave from the monolayer region when the number of phospholipids increases and vice versa, such that the interfacial tension changes are buffered. On the other hand, CE is present in the monolayer region with all phospholipid concentration decreasing the interfacial tension. For quantitative considerations, it should be noted that the buffering region in the used model extends to too small an area per molecule compared to experiments (see recent simulation study in Ollila et al. (9)).

The origin of the lower interfacial tension in the systems containing CE seems to be the positive peak of the pressure profile inside a lipid droplet, and is next to the interfacial

region (see Fig. 3). The peak clearly decreases when TG is introduced into the system. However, it is more difficult to understand the physical origin of this because the peak arises from a complex sum of different interactions. Another possible explanation for the results could be the increase of volume and the water-accessible hydrophobic surface of the droplet due to replacement of CE by TG. However, this cannot explain the difference between systems S6 and S8, and the differences are so small that it is probably not the main reason.

We decided to ensure that the used model gives the same prediction also for planar interface because the interfacial tension in those is experimentally measurable (6). For this purpose, we simulated flat TG-water and CE-water interfaces covered with POPC monolayer having a different area per molecules. The surface pressure area isotherms were calculated by using a trilayer setup as in a recent study (9), and are shown in Fig. S2 in the Supporting Material. The results in Fig. S2 contain the same qualitative features as the results for small lipid droplets because the interfacial tensions are higher for TG systems compared to CE systems. Thus, our prediction should hold also for flat interfaces and systems with lower curvatures, like LDL and VLDL particles.

The interfacial tension is relatively high in all the particles studied here. This means that droplets with the compositions studied in this work would not be thermodynamically stable. However, they might be kinetically stabilized by an energy barrier, which has to be overcome before fusing with other droplet. For further discussion see the next section and Ollila et al. (9).

Influence of ApoA-I protein

The analysis above was conducted for the lipid droplets without proteins. However, physiological lipid droplets are usually covered by a number of proteins having an important role in their functionality, which is the case in HDL as well. To elucidate the effect of apoA-I on the surface of HDL-like lipid droplets, we embedded two and four apoA-Is in the surface of an S2 droplet system. As for the droplets without apoA-Is, we calculated the number of core lipids at the surface and interfacial tensions.

From Fig. 2 we see that the number of polar parts of CE in the vicinity of water phase decreased with increased amount of apoA-Is in the droplets. Comparison among systems S2, SP2, and SP4 suggests that one apoA-I excludes ~6 CEs from the surface. This means that two apoA-Is would exclude 35% of interfacial CEs—i.e., close to their interfacial coverage, calculated to be roughly 30% in the previous work (9).

Also, interfacial tension is decreasing due to addition of apoA-I proteins. However, the decrease is not linear, because the addition of two interfacial proteins causes decrease of 5 mN/m whereas addition of four causes decrease of 15 mN/m. The decrease of interfacial tension due to addition of two apoA-I proteins is slightly larger than 2 mN/m in previous calculations (9). Plausible explanation for the small difference between these studies is that, in previous work, the droplets with proteins also contained TG molecules, which seems to reduce interfacial tension changes. In the previous study, we suggested that, despite a significant surface coverage, the addition of two proteins does not change lipid monolayer properties nor decrease the interfacial tension due to the attraction between phospholipids and protein (interfacial tension antagonism effect) (9). These results suggest the addition of two extra proteins causes a more drastic decrease in interfacial tension. Two extra proteins also significantly increase order parameters of POPC acyl chains, as seen in Fig. 3, which indicates a higher packing of monolayer. In conclusion, we suggest that two or fewer proteins have a slight influence on interfacial tension due to the interfacial tension antagonism effect whereas addition of more proteins starts to decrease interfacial tension due to higher packing of monolayer. Interfacial tension changes induced by C46 and N44 fragments of apoA-I peptides in PC/TG droplets as a function of initial surface pressure were recently measured by Mitsche and Small (11). The surface pressure of S2 droplet before protein addition was 6 mN/m in our simulation. According to the experiments by Mitsche and Small (11), the N44 and C46 segments would decrease the interfacial tension (increase surface pressure) by ~8 mN/m and ~13 mN/m, respectively. These results are in good agreement with our calculated values, even though the experiments are not directly comparable to the simulations because the experiments are done for essentially flat interfaces in equilibrium adsorption conditions.

The surface pressure for HDL_3 particles has been estimated by using surface pressure-area isotherms for lipids and exclusion pressures for proteins, and estimations vary between 20 mN/m and 33 mN/m (33–35). A previous simulation study reported 12 mN/m for HDL with two apo-AI proteins (9). Subtracting the calculated interfacial tensions of SP2 and SP4 systems from the interfacial tension of CE oil droplet (simulation S0) gives surface pressures of 11 mN/m $\pm$ 4 and 21 mN/m $\pm$ 4 for SP2 and SP4 systems, respectively. The calculated values are smaller compared to the experimental estimates. The main reasons for this are probably the absence of cholesterol molecules in our simulations and inaccuracies in the used model, as discussed in the previous study (9). All experimentally (33–35) and theoretically (9) determined surface pressure and interfacial tension values for HDL and LDL droplets, including this study, are relatively large. This would suggest that these droplets are kinetically stabilized, not thermodynamically stable. This is possible also in physiological systems because droplets are constantly modified in circulation by different enzymes. The metastable nature of lipoprotein droplets was already discussed in our previous work (9).

Exchange of TGs and CEs between monolayer and core

To study the exchange rate of CEs and TGs from the monolayer region to the core, the surface localization correlation functions for the polar beads of CE and TG molecules (ES and GLY, respectively) were calculated by using Eq. 5. The correlation functions are shown in Fig. 5 and the related correlation times, calculated by using Eq. 6, are shown in Table 2. The correlation times are roughly an order of magnitude longer for TGs compared to CEs, implying that the exchange of surface TGs is much slower compared to CEs. This means that the energy barrier for transferring TG between core and interface is higher compared to the one for CE.

The slowest correlation functions in Fig. 5 reach zero values roughly in 2 μs, which indicates that this should be a minimum simulation time for this kind of systems. Our results suggest that the TG molecule spends 7–8 times longer on average in the interface compared to CE, which might be relevant for the diffusion of molecules into CETP.

CONCLUSIONS

In this work we have studied the amount of surface-located core lipids and interfacial tension of HDL-like lipid droplets as a function of core and interfacial lipid compositions. Furthermore, we studied the effect of apoA-I molecules to these properties. The study was done by using molecular dynamics simulations with the coarse-grained MARTINI force field.

Because there are 25–50% more TGs and they spend, on average, 7–8 times longer in the vicinity of water phase compared to CE, the relative rate of an enzyme to transport or hydrolyze TGs should be higher compared to CE. This suggests that, for example, CETP could prefer the exchange TGs over CEs even when the ratio of CEs and TGs in the lipoprotein would be equal, or even less. The relative solubility of TGs and CEs into a monolayer is in agreement with the experiments on lipid emulsion by Miller et al. (12). In addition, CEs can replace TGs at the surface to some extent, providing an explanation as to why the addition of CEs to phospholipid-TG systems decreased the lipolysis rate of TGs by lipoprotein lipase (36).

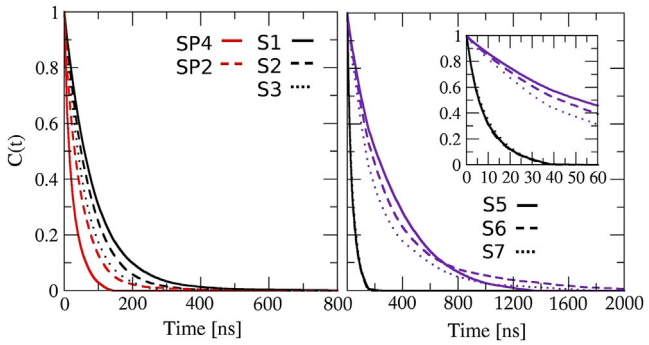

FIGURE 5 Autocorrelation functions for the contacts between W-ES (*black* or *red*) and W-GLY (*purple*) beads.

TABLE 2 Calculated mean surface localization times for CE and TG in different simulations based on autocorrelation functions

System	τ_{CE} (ns)	τ_{TG} (ns)
S1	88	—
S2	72	—
S3	56	—
S5	36	296
S6	36	292
S7	36	236
SP2	48	—
SP4	24	—

The mean interfacial times are given as effective MARTINI time (the real simulation time multiplied by four).

The density in the monolayer region and the number of polar groups in the vicinity of water decreased for core lipids with an increasing number of POPC molecules in all systems, as expected. Interestingly, the decrease was more pronounced for TG than CE molecules in the systems with a mixed CE/TG core. This suggests that the chemical potential increase in the interfacial region due to increasing amount of POPC is more substantial for TG than for CE. On the other hand, the exchange of TG molecules between monolayer and core regions was clearly slower compared to CE molecules. This indicates a higher energy barrier associated with the transfer of TG molecules between interface and core compared to CE molecules.

Expectedly, the interfacial tension also decreased when the number of POPC molecules was increased. The decrease was more pronounced in the systems with the pure CE core compared to the mixed CE-TG core systems. With pure TG core the interfacial tension seems to be essentially unchanged even though the number of POPCs is increased from 0 to 140. The protein-induced decrease in interfacial tension was also slightly higher than in the previous study where the core contained more TG (9). The results are in qualitative agreement with the experiments even thought some quantitative differences exists (6,9). In conclusion, we suggest that the presence of CE in a lipid droplet core decreases the interfacial tension and makes it more dependent on surfactant lipid concentration. These suggestions could be tested with the experimental setup, combining droplet tensiometer and Langmuir trough, as presented in Mitsche et al. (6).

Interesting physiologically relevant hypothesis can be formulated based on our results. Regarding lipoprotein metabolism, lipoprotein particles are constantly remodeled in circulation or taken up by the cell-by-cell surface receptors. Many of these processes are regulated by surface properties, like interfacial lipid content and interfacial tension, of

lipoprotein particles. To demonstrate the potential importance of our results at the physiological level we present three practical examples, where we employ our findings:

1. Our findings suggest that core lipid lipolysis can be regulated by the lipid and apolipoprotein composition because it is well known that the surface concentration of core lipids is important for the activity of various lipolysing agents, such as lipoprotein lipase (36).
2. We suggest that TG molecules are more accessible for CETP compared to CEs. This may favor the transportation of TGs over CEs by CETP, even when the concentrations of TGs and CEs are equal.
3. We suggest that CE lowers the interfacial tension (more stable droplets) while TG buffers the interfacial tension changes due to the composition changes of the surface monolayer. For example, the core lipid composition changes from a TG-rich to a CE-rich core during the conversion of VLDL into LDL in circulation. Based on our results, we suggest that the higher CE fraction makes the surface pressure of LDL particles more sensitive to the variations in monolayer compared to VLDL particles. On the other hand, assuming a constant area per phospholipid during the conversion, the surface pressure of the LDL particle would be higher than the surface pressure of the VLDL due to a higher fraction of CE. This would stabilize the particle and decrease the binding of apolipoproteins to the surface of the LDL particles.

In addition to the discussed topics, the surface pressure of lipoprotein particles can modulate the conformation of surface-bound apolipoproteins as was proposed by Wang et al. (37). However, this topic is not discussed in this work.

SUPPORTING MATERIAL

Additional information for the construction of simulation systems, and the surface tension calculation results for the planar simulations are available at http://www.biophysj.org/biophysj/supplemental/S0006-3495(13)00366-4.

We thank the IT Center for Science in Finland, for providing computational resources for the study. SO acknowledges the Alfred Kordelin, Magnus Ehrnrooth, and Oskar Huttunen Foundations for financial support.

REFERENCES

1. Lund-Katz, S., L. Liu, …, M. C. Phillips. 2003. High density lipoprotein structure. *Front. Biosci.* 8:d1044–d1054.
2. Tsompanidi, E. M., M. S. Brinkmeier, …, K. E. Kypreos. 2010. HDL biogenesis and functions: role of HDL quality and quantity in atherosclerosis. *Atherosclerosis.* 208:3–9.
3. Mahley, R. W., T. L. Innerarity, …, K. H. Weisgraber. 1984. Plasma lipoproteins: apolipoprotein structure and function. *J. Lipid Res.* 25:1277–1294.
4. Small, D. M., L. Wang, and M. A. Mitsche. 2009. The adsorption of biological peptides and proteins at the oil/water interface. A potentially important but largely unexplored field. *J. Lipid Res.* 50(*Suppl*): S329–S334.
5. Ibdah, J. A., K. E. Krebs, and M. C. Phillips. 1989. The surface properties of apolipoproteins A-I and A-II at the lipid/water interface. *Biochim. Biophys. Acta.* 1004:300–308.
6. Mitsche, M. A., L. Wang, and D. M. Small. 2010. Adsorption of egg phosphatidylcholine to an air/water and triolein/water bubble interface: use of the 2-dimensional phase rule to estimate the surface composition of a phospholipid/triolein/water surface as a function of surface pressure. *J. Phys. Chem. B.* 114:3276–3284.
7. Kulovesi, P., J. Telenius, …, J. M. Holopainen. 2010. Molecular organization of the tear fluid lipid layer. *Biophys. J.* 99:2559–2567.
8. Meyers, N. L., L. Wang, and D. M. Small. 2012. Apolipoprotein C-I binds more strongly to phospholipid/triolein/water than triolein/water interfaces: a possible model for inhibiting cholesterol ester transfer protein activity and triacylglycerol-rich lipoprotein uptake. *Biochemistry.* 51:1238–1248.
9. Ollila, O. H. S., A. Lamberg, …, I. Vattulainen. 2012. Interfacial tension and surface pressure of high density lipoprotein, low density lipoprotein, and related lipid droplets. *Biophys. J.* 103:1236–1244.
10. Ouimet, M., and Y. L. Marcel. 2012. Regulation of lipid droplet cholesterol efflux from macrophage foam cells. *Arterioscler. Thromb. Vasc. Biol.* 32:575–581.
11. Mitsche, M. A., and D. M. Small. 2011. C-terminus of apolipoprotein A-I removes phospholipids from a triolein/phospholipids/water interface, but the N-terminus does not: a possible mechanism for nascent HDL assembly. *Biophys. J.* 101:353–361.
12. Miller, K. W., and D. M. Small. 1983. Triolein-cholesteryl oleate-cholesterol-lecithin emulsions: structural models of triglyceride-rich lipoproteins. *Biochemistry.* 22:443–451.
13. Hamilton, J. A., K. W. Miller, and D. M. Small. 1983. Solubilization of triolein and cholesteryl oleate in egg phosphatidylcholine vesicles. *J. Biol. Chem.* 258:12821–12826.
14. Perugini, M. A., P. Schuck, and G. J. Howlett. 2002. Differences in the binding capacity of human apolipoprotein E3 and E4 to size-fractionated lipid emulsions. *Eur. J. Biochem.* 269:5939–5949.
15. Marrink, S. J., H. J. Risselada, …, A. H. de Vries. 2007. The MARTINI force field: coarse grained model for biomolecular simulations. *J. Phys. Chem. B.* 111:7812–7824.
16. Monticelli, L., S. K. Kandasamy, …, S.-J. Marrink. 2008. The MARTINI coarse-grained force field: extension to proteins. *J. Chem. Theory Comput.* 4:819–834.
17. Vuorela, T., A. Catte, …, I. Vattulainen. 2010. Role of lipids in spheroidal high density lipoproteins. *PLOS Comput. Biol.* 6:e1000964.
18. Ollila, O. H. S., H. J. Risselada, …, S. J. Marrink. 2009. 3D pressure field in lipid membranes and membrane-protein complexes. *Phys. Rev. Lett.* 102:078101.
19. Yetukuri, L., S. Söderlund, …, M. Oresic. 2010. Composition and lipid spatial distribution of HDL particles in subjects with low and high HDL-cholesterol. *J. Lipid Res.* 51:2341–2351.
20. Huang, R., R. A. Silva, …, W. S. Davidson. 2011. Apolipoprotein A-I structural organization in high-density lipoproteins isolated from human plasma. *Nat. Struct. Mol. Biol.* 18:416–422.
21. Humphrey, W., A. Dalke, and K. Schulten. 1996. VMD: visual molecular dynamics. *J. Mol. Graph.* 14:33–38, 27–28.
22. Hess, B., C. Kutzner, …, E. Lindahl. 2008. GROMACS 4: algorithms for highly efficient, load-balanced, and scalable molecular simulation. *J. Chem. Theory Comput.* 4:435–447.
23. Berendsen, H. J. C., J. P. M. Postma, …, J. R. Haak. 1984. Molecular dynamics with coupling to an external bath. *J. Chem. Phys.* 81:3684–3690.
24. Dorset, D. L. 1990. Binary phase behavior of cholesteryl oleate with cholesteryl linoleate. *Biochim. Biophys. Acta.* 1046:57–63 (BBA).
25. Kabalnov, A., J. Weers, …, T. Tarara. 1995. Phospholipids as emulsion stabilizers. 1. Interfacial tensions. *Langmuir.* 11:2966–2974.
26. Pregetter, M., R. Prassl, …, P. Laggner. 1999. Microphase separation in low density lipoproteins. Evidence for a fluid triglyceride core below the lipid melting transition. *J. Biol. Chem.* 274:1334–1341.

27. Yetukuri, L., I. Huopaniemi, …, M. Orešič. 2011. High density lipoprotein structural changes and drug response in lipidomic profiles following the long-term fenofibrate therapy in the FIELD substudy. *PLoS ONE.* 6:e23589.

28. Spooner, P. J., J. A. Hamilton, …, D. M. Small. 1986. The effect of free cholesterol on the solubilization of cholesteryl oleate in phosphatidylcholine bilayers: a ^{13}C-NMR study. *Biochim.Biophys. Acta. Biomembr.* 860:345–353.

29. Spooner, P. J. R., and D. M. Small. 1987. Effect of free cholesterol on incorporation of triolein in phospholipid bilayers. *Biochemistry.* 26:5820–5825.

30. Koivuniemi, A., M. Heikelä, …, M. T. Hyvönen. 2009. Atomistic simulations of phosphatidylcholines and cholesteryl esters in high-density lipoprotein-sized lipid droplet and trilayer: clues to cholesteryl ester transport and storage. *Biophys. J.* 96:4099–4108.

31. Ledford, A. S., V. A. Cook, …, R. B. Weinberg. 2009. Structural and dynamic interfacial properties of the lipoprotein initiating domain of apolipoprotein B. *J. Lipid Res.* 50:108–115.

32. Jandacek, R. J., M. R. Webb, and F. H. Mattson. 1977. Effect of an aqueous phase on the solubility of cholesterol in an oil phase. *J. Lipid Res.* 18:203–210.

33. Ibdah, J. A., S. Lund-Katz, and M. C. Phillips. 1989. Molecular packing of high-density and low-density lipoprotein surface lipids and apolipoprotein A-I binding. *Biochemistry.* 28:1126–1133.

34. Slotte, J. P., and L. Grönberg. 1990. Oxidation of cholesterol in low density and high density lipoproteins by cholesterol oxidase. *J. Lipid Res.* 31:2235–2242.

35. Weinberg, R. B., J. A. Ibdah, and M. C. Phillips. 1992. Adsorption of apolipoprotein A-IV to phospholipid monolayers spread at the air/water interface. A model for its labile binding to high density lipoproteins. *J. Biol. Chem.* 267:8977–8983.

36. Demel, R. A., and R. L. Jackson. 1985. Lipoprotein lipase hydrolysis of trioleylglycerol in a phospholipid interface. Effect of cholesteryl oleate on catalysis. *J. Biol. Chem.* 260:9589–9592.

37. Wang, L., M. T. Walsh, and D. M. Small. 2006. Apolipoprotein B is conformationally flexible but anchored at a triolein/water interface: a possible model for lipoprotein surfaces. *Proc. Natl. Acad. Sci. USA.* 103:6871–6876.